Available at
http://pvamu.edu/aam
Appl. Appl. Math.
ISSN: 1932-9466

Applications and Applied Mathematics:
An International Journal
(AAM)

Vol. 15, Issue 2 (December 2020), pp. 1149 - 1171

Effect of porosity on unsteady MHD convection flow Past a moving vertical plate with ramped wall temperature

U.S. Rajput and Mohammad Shareef

Department of Mathematics and Astronomy
University of Lucknow
Lucknow-226007, India
E-mail: rajputshareeflu@gmail.com

Received: July 15, 2019; Accepted: March 7, 2020

Abstract

The unsteady MHD convective flow of an electrically conducting fluid embedded in a porous medium along moving infinite vertical plate with ramped wall temperature and radiation in a rotating system is investigated here. The fluid taken is incompressible and viscous. The governing PDE's of the model are solved by using integral transform method. The analytical solutions for the velocity, concentration and temperature are obtained. The expressions for skin friction, rate of mass transfer and heat transfer near the plate are obtained. The effects of various parameters like porosity of the medium, magnetic field, Soret number, thermal radiation, rotation, radiation and Hall current on the flow field are discussed. It is observed that velocity increases with the increase in the porosity parameter *K*. It reveals that a porous medium having large permeability supports the movement of the fluid in the system. Also, it is noticed that Hall parameter reduces the resistive effect of the applied magnetic field. Such a study assumes importance because both rotation and Hall current induce secondary flow in the flow-field. The results of the research may be useful in many industrial applications.

Keywords: MHD; Soret effect; Ion Slip; Hall current; Rotation; Porous medium; Radiation

MSC 2010: 76U05, 76S05, 76W05, 76E06

1. Introduction

Unsteady convection flows of viscous incompressible fluids past semi-infinite or infinite vertical flat surfaces have been investigated by many researchers due to their technological requirements.

Flow past a semi-infinite vertical plate was first investigated by Pohlhausen (1921) who solved it by integral method. Ostrach (1953) solved the same problem by similarity method. Transient convective flow past a semi-infinite vertical plate was studied by Siegel (1958). Gebhart (1961) analysed the same problem by using an approximate method.

Convective heat and mass transfer from a body with different geometries embedded in a saturated or unsaturated porous medium has many applications in engineering and science such as thermal insulators, solidification of binary alloys and crystal growth dispersion of dissolved materials.

Extensive researches on thermal and species convection through a porous media under the influence of magnetic field are presented by Agarwal *et al*. (1983), Branover (1978), Osalusi and Sibanda (2006), Watanabe and Pop (1994), Nield and Bejan (2006), Michiyochi *et al.* (1976) , Muthucumaraswamy and Prema (2016), Mazumdar *et al*. (1976), Attia (2005, 2009), Pop and Ingham (2002), Cowling (1957), Vajravelu and Nayfeh (1992), Jaimala *et al*. (2013), Vafai (2005), Riley (1976), Sparrow and Cess (1961) etc. In 2017 Sheikh *et al.* compared the solution of generalized Casson fluid model with heat generation and chemical reaction. They (2017) solved the model by Atangana-Baleanu and Caputo-Fabrizio derivative technique and observed that velocities increase gradually with time. Further Sheikh *et al.* (2018) used Atangana-Baleanu fractional derivative technique to theoretically analyze the performance of a solar collector using CeO_2 and Al_2O_3 water based nanofluids with inclined plate. Recentely, heat transfer analysis in the flow of ethylene glycol-based Molybdenum disulfide generalized nanofluid (EGMDGN) over an isothermal vertical plate with heat transfer was done by Ali *et al.* (2019).

In many flows heat and mass transfer take place simultaneously having an effect on each other and leading to the thermal-diffusion and diffusion-thermo effects. Such problems related to diffusion-themo (Dufour) and thermal-diffusion (Soret) effects have been examined in different physical condition by EL-Kabeir *et al.* (2010), Chamkha *et al.* (2013), Chamkha and Rashad (2014), Gangadhar (2013), Reddy and Rao (2012), Rani and Reddy (2013), Beg *et al.* (2009), Postelnicu (2007), Kafoussias and Williams (1995), Bhargava *et al.* (2009), Alam and Rahman (2006), Anghel (2000), Makinde (2011), Ibrahim (2009) and others.

Further, the rotating fluids have great geophysical and astrophysical uses. Some natural phenomena involve rotating flows with heat and mass transfer like hurricanes tornadoes, ocean circulation currents, geophysical systems, etc. Various articles related to rotating flows have been published: (Greenspan (1968), Owen and Rogers (1959), Soong and Ma (1995), Soong (2001), Muthucumaraswamy *et al.* (2013)).

Motivated by the above mentioned researches and their enormous applications, we extend our previous work (2018) to analyze the radiation and porosity effect under different moving conditions on unsteady MHD free convection flow past a moving vertical plate with ramped wall temperature. The time dependent, nonlinear and coupled governing equations of the model are obtained and solved by using Laplace transform scheme. The influence of different flow parameters on the concentration, temperature and transient velocity, as well as heat and mass transfer rates is analyzed.

2. Mathematical analysis

Consider a coordinate system such that an infinite plate is lying in $z = 0$ plane and a magnetic field $\vec{B} = (0, 0, B_o)$ is applied normal to the plate i.e. along z– axis. Both the plate and fluid are in a state of rigid body rotation with uniform angular velocity $\vec{\Omega} = (0, 0, \Omega)$ about z – axis (as illustrated in Figure 1). Initially, the plate is at rest with a uniform temperature and concentration T_∞ and C_∞ respectively.

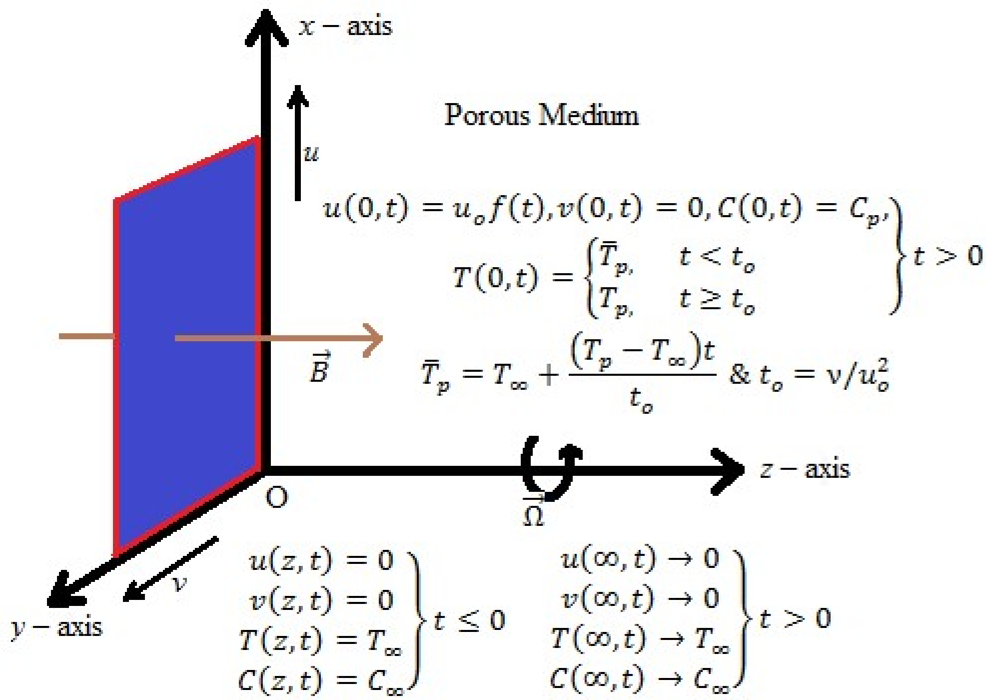

Figure 1. Geometry of the Problem

At time $t > 0$, the plate suddenly begins to move vertically upward in its own plane in positive x direction with a velocity $u_o f(t)$ and concentration are lowered or raised to C_p. At the same time the plate temperature is changed to $T_\infty + (T_p - T_\infty) t / t_o$ $(0 < t < t_o)$ and T_p $(t \geq t_o)$. The movement of the plate and the free convection cause the fluid motion. The model governs the coupled and non-linear PDEs. However, within the boundary layer general behaviour of the fluid motion can be examined by simplified problem with some assumptions, stipulated below.

i) The fluid far away from the plate is undisturbed.

ii) The plate is of infinite extent, so all the physical variables can be considered as a function of t and z only.

iii) No polarization or applied voltages exist.

iv) The fluid has small value of magnetic Reynolds number; hence the induced magnetic field can be neglected.

v) All the fluid properties are constants and the variation in density is neglected everywhere except in the buoyancy term.

vi) In the generalized Ohm's law, effect of Hall currents is taken into account and thermoelectric effect and ion-slip are neglected.

vii) The plate is electrically non-conducting.

The governing equations of a viscous, incompressible and electrically conducting fluid under the above said assumptions are:

Energy transport equation

$$\frac{\partial T}{\partial t}=\frac{k}{\rho c_p}\frac{\partial^2 T}{\partial z^2}-\frac{1}{\rho c_p}\frac{\partial q^{(r)}}{\partial z}. \tag{1}$$

Mass transport equation

$$\frac{\partial C}{\partial t}=D\frac{\partial^2 C}{\partial z^2}+\frac{D_T k_T}{T_m}\frac{\partial^2 T}{\partial z^2}. \tag{2}$$

Momentum transport equation

$$\frac{\partial u}{\partial t}-2\Omega v=\upsilon\frac{\partial^2 u}{\partial z^2}+g\beta(T-T_\infty)+g\beta^*(C-C_\infty)+\frac{B_o}{\rho}j_y-\frac{\upsilon}{K}u, \tag{3}$$

$$\frac{\partial v}{\partial t}+2\Omega u=\upsilon\frac{\partial^2 v}{\partial z^2}-\frac{B_o}{\rho}j_x-\frac{\upsilon}{K}v, \tag{4}$$

where

$$j_x=\frac{\sigma B_o\{(1+m\,m_i)v+m\,u\}}{(1+m\,m_i)^2+m^2},\quad j_y=\frac{\sigma B_o\{m\,v-(1+m\,m_i)u\}}{(1+m\,m_i)^2+m^2}.$$

Notation and symbols-

D Mass diffusion coefficient

K Permeability parameter of the medium

g Acceleration due to gravity

m_i Ion-slip parameter

D_T Thermal diffusion coefficient

u Component of the fluid velocity along x- axis (primary velocity)
v C of the fluid velocity along y- axis (secondary velocity)
C Concentration at any time t in the fluid
T Temperature at any time t in the fluid
ρ Density of the fluid
m Hall parameter
ν Kinematic viscosity of the fluid
σ Electric conductivity of the fluid
T_m Mean fluid temperature
k_T Thermal diffusion ratio
β^* Volumetric coefficient of concentration expansion
k Thermal conductivity of the fluid
β Volumetric coefficient of thermal expansion
c_p Heat capacity of the fluid

The admissible initial and boundary conditions are taken as

for $t \leq 0$: $u = v = 0$,

$T = T_\infty, C = C_\infty$,

for all z and for $t > 0$:

$u = u_1, v = 0$,

$C = C_\infty$,

$T = T_1$ at $z = 0$ and

$$u \to 0,\ v \to 0, T \to T_\infty,\ C \to C_\infty \text{ as } z \to \infty, \tag{5}$$

where

$$u_1 = u_o f\left(t\right),\ T_1 = \begin{cases} T_\infty + \left(T_p - T_\infty\right)\dfrac{t}{t_o},\ t \leq t_o \\ T_p,\ \ t > t_o \end{cases} \text{ and } t_o = \frac{\upsilon}{u_o^2}.$$

The radiative heat flux $q^{(r)}$ can take form (Rosseland appro. (Brewster (1992))

$$q^{(r)} = -\frac{4\sigma_s}{3k_e}\frac{\partial T^4}{\partial z}, \tag{6}$$

where σ_s and k_e are the Stefan-Boltzmann constant and mean absorption coefficient respectively.

Considering the temperature difference within the flow very small, we can take T^4 as

$$T^4 \cong 4T_\infty^3 T - 3T_\infty^4 \text{ (Neglecting higher order terms in Taylor expansion),} \tag{7}$$

with the help of (6) and (7), (1) takes form

$$\frac{\partial T}{\partial t} = \alpha \frac{\partial^2 T}{\partial z^2} + \frac{16\sigma_s \alpha T_o^3}{3k_e k} \frac{\partial^2 T}{\partial z^2}. \tag{8}$$

For changing the above equations into non-dimensional form, following non-dimensional parameters and variables are taken:

$$\begin{aligned} &u^* = \frac{u}{u_o}, v^* = \frac{v}{u_o}, t^* = \frac{u_o^2}{\upsilon} t,\ z^* = \frac{u_o}{\upsilon} z,\ \omega^* = \frac{\upsilon}{u_o^2}\omega, \\ &\theta = \frac{(T - T_\infty)}{(T_p - T_\infty)},\ \phi = \frac{(C - C_\infty)}{(C_p - C_\infty)},\ S_c = \frac{\upsilon}{D}, P_r = \frac{\upsilon}{\alpha}, \\ &\Omega^* = \frac{\upsilon}{u_o^2}\Omega,\ K^* = \frac{u_o^2}{\upsilon^2} K,\ G_r = \frac{g\beta\upsilon(T_p - T_\infty)}{u_o^3}, \\ &G_m = \frac{g\beta^{**}\upsilon(C_p - C_\infty)}{u_o^3},\ S_r = \frac{D_T k_T (T_p - T_\infty)}{T_m \upsilon (C_p - C_\infty)}. \end{aligned} \tag{9}$$

By using equation (9), equations (2), (3), (4), (5) and (8), change to

$$\frac{\partial \theta}{\partial t^*} = \frac{1}{R_a P_r} \frac{\partial^2 \theta}{\partial z^{*2}}, \tag{10}$$

$$\frac{\partial \phi}{\partial t^*} = \frac{1}{S_c} \frac{\partial^2 \phi}{\partial z^{*2}} + S_r \frac{\partial^2 \theta}{\partial z^{*2}}, \tag{11}$$

$$\frac{\partial u^*}{\partial t^*} - 2\Omega^* v^* = \frac{\partial^2 u^*}{\partial z^{*2}} + \frac{M}{(1 + m\, m_i)^2 + m^2} \{m\, v^* - (1 + m\, m_i) u^*\} + G_r \theta + G_m \phi - \frac{u^*}{K^*}, \tag{12}$$

$$\frac{\partial v^*}{\partial t^*} + 2\Omega^* u^* = \frac{\partial^2 v^*}{\partial z^{*2}} - \frac{M}{(1 + m\, m_i)^2 + m^2} \{(1 + m\, m_i) v^* + m\, u^*\} - \frac{v^*}{K^*}, \tag{13}$$

for $t^* \le 0$: $u^* = v^* = 0,\ \theta = 0,\ \phi = 0,$

for all z^* and for $t^* > 0 : u^* = \overline{u}_1,\ v^* = 0,\ \phi = 1,\ \theta = \overline{T}_1$ at $z^* = 0,$

and

$$u^* \to 0,\ v^* \to 0,\ \theta \to 0,\ \phi \to 0 \text{ as } z^* \to \infty, \tag{14}$$

where

$$\bar{u}_1 = f\left(t^*\right),\ \bar{T}_1 = \begin{cases} t^*, & t^* \le 1 \\ 1, & t^* > 1 \end{cases},\ R_a = \frac{3R}{3R+4},\ R = \frac{k_e k}{4\sigma_s T_o^3} \text{ and } M = \frac{\sigma B_o^2\ \upsilon}{\rho u_o^2}.$$

For equations (12) and (13), put $u^* + iv^* = V^*$ ($i = \sqrt{-1}$), we get the simplified form of the equation as

$$\frac{\partial V^*}{\partial t^*} = \frac{\partial^2 V^*}{\partial z^{*2}} - bV^* + G_r\theta + G_m\phi, \tag{15}$$

and boundary conditions (14) changes to

$$\begin{aligned} &\text{for } t^* \le 0:\ V^* = 0,\ \theta = 0,\ \phi = 0 \text{ for all } z^* \\ &\text{and} \\ &\text{for } t^* > 0: V^* = \bar{u}_1,\ \phi = 1,\ \theta = \bar{T}_1 \text{ at } z^* = 0 \text{ and } V^* \to 0, \\ &\theta \to 0,\ \phi \to 0 \text{ as } z^* \to \infty, \end{aligned} \tag{16}$$

where $\bar{u}_1 = f\left(t^*\right),\ \bar{T}_1 = \begin{cases} t^*, & t^* \le 1 \\ 1, & t^* > 1 \end{cases}$.

Notation and symbols-

G_m Mass Grashof number

G_r Thermal Grashof number

α Thermal diffusivity

S_c Schmidt number

K^* Dimensionless permeability parameter

v^* Dimensionless secondary velocity of the fluid

u^* Dimensionless primary velocity of the fluid

t^* Dimensionless time

M Magnetic field parameter

P_r Prandtl number

S_r Soret number

z^* Dimensionless spatial coordinate normal to the plate

θ Dimensionless temperature

ϕ Dimensionless concentration

Ω^* Dimensionless rotation parameter

R Radiation parameter

Without loss of generality, after removing the star (*), the above set of equations reduce to

$$\frac{\partial \theta}{\partial t} = \frac{1}{R_a P_r} \frac{\partial^2 \theta}{\partial z^2}, \tag{17}$$

$$\frac{\partial \phi}{\partial t} = \frac{1}{S_c} \frac{\partial^2 \phi}{\partial z^2} + S_r \frac{\partial^2 \theta}{\partial z^2}, \tag{18}$$

$$\frac{\partial V}{\partial t} = \frac{\partial^2 V}{\partial z^2} - bV + G_r \theta + G_m \phi, \tag{19}$$

with boundary conditions

for $t \leq 0$: $V = 0,\ \theta = 0,\ \phi = 0$ for all z

and

for $t > 0: V = f(t),\ \phi = 1,\ \theta = \begin{cases} t, & t \leq 1 \\ 1, & t > 1 \end{cases}$ at $z = 0$ and $V \to 0$,

$\theta \to 0,\ \phi \to 0$ as $z \to \infty$, (20)

where $b = \dfrac{M\ i}{m + i(1 + m\ m_i)} + 2i\Omega + \dfrac{1}{K}$.

Applying the Laplace operator to the PDE's (17), (18) and (19), we get a set of ODE's in variables z and s as follows:

$$\frac{d^2}{dz^2} \bar{\theta}(z,\ s) - R_a P_r s \bar{\theta}(z,\ s) = 0, \tag{21}$$

$$\frac{d^2}{dz^2} \bar{\phi}(z,\ s) - S_c s \bar{\phi}(z,\ s) = -S_c S_r \frac{\partial^2 \bar{\theta}(z,\ s)}{dz^2}, \tag{22}$$

$$\frac{d^2}{dz^2} \bar{V}(z,\ s) - (b + s) \bar{V}(z,\ s) = -G_r \bar{\theta}(z,s) - G_m \bar{\phi}(z,s), \tag{23}$$

The changed boundary conditions are

$$\bar{V}(0,\ s) = L\{f(t)\},\ \bar{V}(\infty,\ s) = 0, \tag{24}$$

$$\bar{\theta}(0,\ s) = \frac{1 - e^{-s}}{s^2},\ \bar{\theta}(\infty,\ s) = 0, \tag{25}$$

$$\bar{\phi}(0,\ s)=\frac{1}{s},\ \bar{\phi}(\infty,\ s)=0, \tag{26}$$

where Laplace transforms of $V(z,\ t)$, $\theta(z,\ t)$ and $\phi(z,\ t)$ are denoted as $\bar{V}(z,\ s)$, $\bar{\theta}(z,\ s)$ and $\bar{\phi}(z,\ s)$ respectively.

By using equation (25) into equation (21), we get

$$\bar{\theta}(z,\ s)=\frac{(1-e^{-s})}{s^2}e^{-z\sqrt{sP_rR_a}} \tag{27}$$

or

$$\theta(z,\ t)=L^{-1}\left\{\frac{e^{-z\sqrt{sP_rR_a}}}{s^2}\right\}-L^{-1}\left\{e^{-s}\left(\frac{e^{-z\sqrt{sP_rR_a}}}{s^2}\right)\right\}.$$

By using the characteristic of inverse Laplace transform:

If $L^{-1}\{G(s)\}=g(t)$, then $L^{-1}\{e^{-ks}G(s)\}=g(t-k)H(t-k)$

and the equation (27) gives the temperature profile

$$\theta(z,\ t)=\theta_1(z,\ t)-\theta_1(z,\ t-1)H(t-1), \tag{28}$$

where

$$\theta_1(z,\ t)=L^{-1}\left\{\frac{e^{-z\sqrt{sP_rR_a}}}{s^2}\right\}=-ze^{-\frac{z^2P_rR_a}{4t}}\frac{\sqrt{tP_rR_a}}{\sqrt{\pi}}+\left(t+\frac{z^2P_rR_a}{2}\right)Erfc\left(\frac{z\sqrt{P_rR_a}}{2\sqrt{t}}\right),$$

here L^{-1} indicates the inverse Laplace transform, $H(t-1)$ is the Heaviside unit step function and $Erfc(.)=1-Erf(.)$ is the complimentary error function.

Now to obtain the solution for the concentration, we substitute equation (27) into equation (22), and then using the boundary conditions (26), we get

$$\bar{\phi}(z,\ s)=\left(\frac{e^{-z\sqrt{sS_c}}}{s}\right)+a\frac{(1-e^{-s})}{s^2}\left(e^{-z\sqrt{sP_rR_a}}-e^{-z\sqrt{sS_c}}\right) \tag{29}$$

or

$$\phi(z,\ t)=L^{-1}\left(\frac{e^{-z\sqrt{sS_c}}}{s}\right)+aL^{-1}\left(\frac{e^{-z\sqrt{sP_rR_a}}-e^{-z\sqrt{sS_c}}}{s^2}\right)-aL^{-1}\left\{e^{-s}\left(\frac{e^{-z\sqrt{sP_rR_a}}-e^{-z\sqrt{sS_c}}}{s^2}\right)\right\}$$

or

$$\phi(z,\ t) = Erfc\left(\frac{z\sqrt{S_c}}{2\sqrt{t}}\right) + a\phi_1(z,\ t) - a\phi_1(z,\ t-1)H(t-1), \tag{30}$$

where

$$a = \frac{P_r S_r S_c R_a}{S_c - P_r R_a}$$

and

$$\phi_1(z,\ t) = L^{-1}\left(\frac{e^{-z\sqrt{sP_rR_a}} - e^{-z\sqrt{sS_c}}}{s^2}\right) = -\left(t + z^2\frac{S_c}{2}\right)Erfc\left(\frac{z\sqrt{S_c}}{2\sqrt{t}}\right)$$
$$-z\sqrt{\frac{t}{\pi}}\left(e^{-\frac{z^2P_rR_a}{4t}}\sqrt{P_rR_a} - e^{-\frac{z^2P_rR_a}{4t}}\sqrt{S_c}\right) + \left(t + \frac{z^2P_rR_a}{2}\right)Erfc\left(\frac{z\sqrt{P_rR_a}}{2\sqrt{t}}\right).$$

Substituting equations (27) and (29) into equation (23), and using the prescribed boundary conditions (24), the solutions for transient velocity for the two cases are obtained as

$$\overline{V}(z,\ s) = e^{-z\sqrt{b+s}}L\{f(t)\} + \frac{A_3}{s(s-B_2)}\left(e^{-z\sqrt{sS_c}} - e^{-z\sqrt{b+s}}\right) + \frac{1-e^{-s}}{s^2}\frac{(A_1+A_2)}{(s-B_1)}\left(e^{-z\sqrt{R_aP_r}} - e^{-z\sqrt{b+s}}\right)$$
$$+\frac{1-e^{-s}}{s^2}\frac{aA_3}{(s-B_2)}\left(e^{-z\sqrt{b+s}} - e^{-z\sqrt{sS_c}}\right)$$

or

$$V(z,\ t) = L^{-1}\left[e^{-z\sqrt{b+s}}L\{f(t)\}\right] + L^{-1}\left\{\frac{A_3}{s(s-B_2)}\left(e^{-z\sqrt{sS_c}} - e^{-z\sqrt{b+s}}\right)\right\}$$
$$+L^{-1}\left\{\frac{aA_3}{s^2(s-B_2)}\left(e^{-z\sqrt{b+s}} - e^{-z\sqrt{sS_c}}\right) + \frac{(A_1+A_2)}{s^2(s-B_1)}\left(e^{-z\sqrt{R_aP_r}} - e^{-z\sqrt{b+s}}\right)\right\}$$
$$-L^{-1}\left[e^{-s}\left\{\frac{aA_3}{s^2(s-B_2)}\left(e^{-z\sqrt{b+s}} - e^{-z\sqrt{sS_c}}\right) + \frac{(A_1+A_2)}{s^2(s-B_1)}\left(e^{-z\sqrt{R_aP_r}} - e^{-z\sqrt{b+s}}\right)\right\}\right],$$

where

$$A_1 = \frac{G_r}{1-P_rR_a}, A_2 = \frac{aG_m}{1-P_rR_a}, A_3 = \frac{G_m}{1-S_c}, B_1 = \frac{b}{P_rR_a - 1} \text{ and } B_2 = \frac{b}{S_c - 1}.$$

Case 1: Motion of the plate with uniform velocity:

Consider $f(t) = H(t)$, So $L[f(t)] = \dfrac{1}{s}$.

Therefore,

$$V(z,\ t)=\frac{1}{2}\left\{2cosh(k_1z)+e^{-k_1z}Erf(k_1\sqrt{t}-\eta)-e^{k_1z}Erf(k_1\sqrt{t}+\eta)\right\}$$
$$+V_o(z,\ t)+V_1(z,\ t)-V_1(z,\ t-1)H(t-1). \tag{31}$$

Case 2: Motion of the plate with periodic acceleration:

Consider $f(\mathrm{t})=Sin\omega t\ H(t)$, So $L\left[f(\mathrm{t})\right]=\dfrac{\omega}{s^2+\omega^2}$.

Therefore,

$$\begin{aligned}V(z,\ t)&=\frac{i}{2}\left\{e^{-i\omega t}cosh(a_1z)-e^{i\omega t}cosh(a_2z)\right\}-\frac{ie^{-i\omega t}}{4}\left\{e^{-a_1z}Erf\left(\eta-a_1\sqrt{t}\right)+e^{a_1z}Erf\left(\eta+a_1\sqrt{t}\right)\right\}\\&+\frac{ie^{i\omega t}}{4}\left\{e^{-a_2z}Erf\left(\eta-a_2\sqrt{t}\right)+e^{a_2z}Erf\left(\eta+a_2\sqrt{t}\right)\right\}\\&+V_o(z,\ t)+V_1(z,\ t)-V_1(z,\ t-1)H(t-1),\end{aligned} \tag{32}$$

here

$$\begin{aligned}V_o(z,\ t)&=L^{-1}\left\{\frac{A_3}{s(s-B_2)}\left(e^{-z\sqrt{sS_c}}-e^{-z\sqrt{b+s}}\right)\right\}\\&=c_1\left\{2Cosh\left(k_1z\right)+e^{-k_1z}Erf\left(k_1\sqrt{t}-\eta\right)-e^{k_1z}Erf\left(k_1\sqrt{t}+\eta\right)\right\}\\&-c_1e^{tB_2}\left\{2Cosh\left(k_2z\right)-e^{-k_2z}Erf\left(\eta-k_2\sqrt{t}\right)-e^{k_2z}Erf\left(\eta+k_2\sqrt{t}\right)\right\}\\&+c_1e^{tk_5^2}\left\{2Cosh\left(k_4z\right)+e^{-k_4z}Erf\left(k_5\sqrt{t}-k_6\eta\right)-e^{k_4z}Erf\left(k_5\sqrt{t}+k_6\eta\right)\right\}-2c_1Erfc\left(k_6\eta\right),\end{aligned}$$

$$\begin{aligned}V_1(z,\ t)&=L^{-1}\left\{\frac{(A_1+A_2)}{s^2(s-B_1)}\left(e^{-z\sqrt{R_aP_r}}-e^{-z\sqrt{b+s}}\right)\right\}+L^{-1}\left\{\frac{aA_3}{s^2(s-B_2)}\left(e^{-z\sqrt{b+s}}-e^{-z\sqrt{sS_c}}\right)\right\}\\&=-c_2e^{k_{10}^2t}\left\{2cosh(k_7z)-e^{-k_7z}Erf(\eta-k_7\sqrt{t})-e^{k_7z}Erf(\eta+k_7\sqrt{t})\right\}\\&+(c_3t+c_4)\left\{2cosh(k_1z)+e^{-k_1z}Erf(k_1\sqrt{t}-\eta)-e^{k_1z}Erf(k_1\sqrt{t}+\eta)\right\}\\&+c_5z\left\{2sinh(k_1z)+e^{-k_1z}Erf(k_1\sqrt{t}-\eta)-e^{k_1z}Erf(k_1\sqrt{t}+\eta)\right\}+c_6z\sqrt{t}e^{-k_8^2\eta^2}\\&+c_2e^{k_{10}^2t}\left\{2cosh(k_9z)+e^{-k_9z}Erf(k_{10}\sqrt{t}-k_8\eta)-e^{k_9z}Erf(k_{10}\sqrt{t}+k_8\eta)\right\}\\&+c_9e^{k_5^2t}\left\{2cosh(k_2z)-e^{-k_2z}Erf(\eta-k_2\sqrt{t})-e^{k_2z}Erf(\eta+k_2\sqrt{t})\right\}\end{aligned}$$

$$-c_9 e^{k_5^2 t}\left\{2cosh(k_4 z)+e^{-k_4 z}Erf(k_5\sqrt{t}-k_6\eta)-e^{k_4 z}Erf(k_5\sqrt{t}+k_6\eta)\right\}$$
$$+(c_{12}z^2+c_{11}t+2c_9)Erfc(k_6\eta)-(c_7 z^2+c_8 t+2c_2)Erfc(k_8\eta)-c_{10}z\sqrt{t}e^{-k_6^2\eta^2},$$

$$a_1=\sqrt{b-i\omega}, a_2=\sqrt{b+i\omega},\ c_1=\frac{A_3}{2B_2}, c_2=\frac{A_1+A_2}{2B_1^2},\ c_3=\frac{A_1+A_2}{2B_1}-\frac{aA_3}{2B_2}, c_4=\frac{A_1+A_2}{2B_1^2}-\frac{aA_3}{2B_2^2},$$

$$c_5=\frac{A_1+A_2}{4B_1\sqrt{b}}-\frac{aA_3}{4B_2\sqrt{b}},\ c_6=\frac{\sqrt{P_rR_a}\left(A_1+A_2\right)}{B_1\sqrt{\pi}}, c_7=\frac{P_rR_a\left(A_1+A_2\right)}{2B_1}, c_8=\frac{A_1+A_2}{B_1},\ c_9=\frac{aA_3}{2B_2^2},$$

$$c_{10}=\frac{aA_3}{B_2}\sqrt{\frac{S_c}{\pi}},\ c_{11}=\frac{aA_3}{B_2},\ c_{12}=\frac{aA_3S_c}{2B_2}, k_1=\sqrt{b},\ k_2=\sqrt{b+B_2},\ k_4=\sqrt{B_2S_c}, k_5=\sqrt{B_2},$$

$$k_6=\sqrt{S_c},\ c_{11}=\frac{aA_3}{B_2},\ c_{12}=\frac{aA_3S_c}{2B_2}, k_1=\sqrt{b},\ k_2=\sqrt{b+B_2},\ k_4=\sqrt{B_2S_c}, k_5=\sqrt{B_2},\ k_6=\sqrt{S_c},$$

$$k_7=\sqrt{b+B_1},\ k_8=\sqrt{P_rR_a}, k_9=\sqrt{B_1P_rR_a},\ k_{10}=\sqrt{B_1},\ \eta=\frac{z}{2\sqrt{t}}.$$

2.1. Nusselt number, Sherwood number and Skin friction coefficient

By using (9), non-dimensional

$$\text{Sherwood number } (Sh)=-\left(\frac{\partial\phi}{\partial z}\right)_{z=0}=\sqrt{\frac{S_c}{\pi t}}+\frac{2a}{\sqrt{\pi}}\left(\sqrt{P_rR_a}-\sqrt{S_c}\right)\left\{\sqrt{t}-\sqrt{t-1}H(t-1)\right\} \quad (33)$$

$$\text{and Nusselt number } (Nu)=-\left(\frac{\partial\theta}{\partial z}\right)_{z=0}=2\sqrt{\frac{P_rR_at}{\pi}}-2\sqrt{\frac{P_rR_a(t-1)}{\pi}}H(t-1). \quad (34)$$

And the skin friction components along *x*-axis and *y*-axis are

$$\tau_x=-\mu\frac{\partial u}{\partial z} \text{ and } \tau_y=-\mu\frac{\partial v}{\partial z} \text{ respectively,}$$

the non-dimensional form (using equation (9) of skin friction can be written as

$$\tau_1\left(z^*,\ t^*\right)=\frac{\tau_x}{\tau_o}=-\frac{\partial u^*}{\partial z^*} \text{ and } \tau_2\left(z^*,\ t^*\right)=\frac{\tau_x}{\tau_o}=-\frac{\partial v^*}{\partial z^*} \text{ where } \tau_o=\rho u_o^2.$$

Take $\tau_1\left(z^*,\ t^*\right)+i\tau_2\left(z^*,\ t^*\right)=\tau\left(z^*,\ t^*\right)$ and after omitting the star (*), the non-dimensional skin friction changes to

$$\tau(z,\ t)=\tau_1(z,\ t)+i\tau_2(z,\ t)=-\frac{\partial V(z,\ t)}{\partial z}.$$

Therefore, the coefficients of skin friction at the plate in complex form is given as

$$\left[S_f(t)\right]_{case1}=\tau(0,\ t)=\frac{e^{-k_1^2 t}}{\sqrt{\pi t}}+k_1 erf\left(k_1\sqrt{t}\right)+S_o(t)+S_1(t)-S_1(t-1)H(t-1), \tag{35}$$

$$\left[S_f(t)\right]_{case2}=\tau(0,\ t)=\frac{1}{2}ie^{-i\omega t}\left\{\frac{e^{-a_1^2 t}}{\sqrt{\pi t}}+a_1 erf\left(a_1\sqrt{t}\right)\right\}-\frac{1}{2}ie^{i\omega t}\left\{\frac{e^{-a_2^2 t}}{\sqrt{\pi t}}+a_2 erf\left(a_2\sqrt{t}\right)\right\}$$
$$+S_o(t)+S_1(t)-S_1(t-1)H(t-1), \tag{36}$$

where

$$S_o(t)=2c_1\left\{\frac{e^{-k_1^2 t}-k_6}{\sqrt{\pi t}}+k_1 Erf\left(k_1\sqrt{t}\right)\right\}-2c_1 e^{B_2 t}\left\{\frac{e^{-k_2^2 t}}{\sqrt{\pi t}}+k_2 Erf\left(k_2\sqrt{t}\right)\right\}$$
$$+2c_1 e^{k_5^2 t}\left\{\frac{k_6 e^{-k_5^2 t}}{\sqrt{\pi t}}+k_4 Erf\left(k_5\sqrt{t}\right)\right\},$$

$$S_1(t)=2c_5 Erf\left(k_1\sqrt{t}\right)-c_6\sqrt{t}+c_{10}\sqrt{t}+2\left(c_3 t+c_4\right)\left\{\frac{e^{-k_1^2 t}}{\sqrt{\pi t}}+k_1 Erf\left(k_1\sqrt{t}\right)\right\}$$
$$+2c_9 e^{k_5^2 t}\left\{\frac{e^{-k_2^2 t}}{\sqrt{\pi t}}+k_2 Erf\left(k_2\sqrt{t}\right)\right\}+\frac{2c_0+tc_{11}}{\sqrt{\pi t}}k_6-2c_9 e^{k_5^2 t}\left\{\frac{k_6 e^{-k_5^2 t}}{\sqrt{\pi t}}+k_4 Erf\left(k_5\sqrt{t}\right)\right\}$$
$$-2c_2 e^{k_{10}^2 t}\left\{\frac{e^{-k_7^2 t}}{\sqrt{\pi t}}+k_7 Erf\left(k_7\sqrt{t}\right)\right\}-\frac{2c_2+tc_8}{\sqrt{\pi t}}k_8+2c_2 e^{k_{10}^2 t}\left\{\frac{k_8 e^{-k_{10}^2 t}}{\sqrt{\pi t}}+k_9 Erf\left(k_{10}\sqrt{t}\right)\right\}.$$

Hence, the coefficients of skin friction in the primary (x-axis) and secondary (y-axis) directions respectively can be obtained as follows:

$$S_{f_x}=Re\left(S_f\right)\ \text{and}\ S_{f_y}=Im\left(S_f\right). \tag{37}$$

3. Results and discussion

The analytical solution of fluid velocity having two components, one along the direction of motion of the plate (primary velocity u), and the other along the transverse direction (secondary velocity v), is displayed graphically in Figures 2 to 7. It is noticed that in both the cases: primary velocity and secondary velocity secure an individual extreme value in the region near the plate and then decrease slowly up to free stream value. The effect of Hall and ion slip parameters on the velocity profile is displayed in Figures.2–4. It is examined that the magnitude of secondary velocity increases gradually with the increase in Hall parameter in the range $0 < m < 2$ and it decreases for $m \geq 2$. This may be referred to the fact that for large value of m, the term

$1/(1+m^2)$ is sufficiently small; so large value of Hall parameter reduces the resistive effect of the applied magnetic field. On the other hand, the primary component of velocity speeds up with the increase in *m*. Figure 4 depicts that for a large and fixed value of magnetic field parameter, the primary velocity speeds up and secondary velocity slows down when m_i is increased. It is because an increase in m_i causes the reduction of the magnetic force on *u*.

In case 2, the effect of Soret number and Schmidt number can be seen from the Figure 7. It is noticed that Soret number enhances the flow while Schmidt number retards the flow. Figures 5–6 depicts the effect of magnetic parameters, permeability parameter and rotation in both the cases. It is found that the secondary velocity increases and primary velocity decreases with increase in the rotation parameter. So, rotation can enhance the secondary flow and reduce the flow along the plate. Physically it may be attributed to the fact that the Coriolis force has a tendency to accelerate the secondary flow and retard the primary flow. It can also be seen that the velocity increases with the increase in *K*; a porous medium having large permeability supports the movement of the fluid through it. While if the magnetic parameter is increased the primary velocity decreases and secondary velocity increases. It is because of the fact that a transverse applied magnetic field causes the Lorentz force which acts in the transverse direction and hence opposes the primary flow. It is evident from Figures. 8–9 that the Skin-Friction components S_{f_x} and S_{f_y} decreases with the increase in K / S_r. While S_{f_x} increases and S_{f_y} decreases with the increase in Ω. Furthermore, dimensionless Schmidt number S_c is defined as the ratio of momentum diffusivity to the mass diffusivity of the fluid and it is observed from the Figure 10 that an increase in S_c causes the reduction of concentration within the boundary layer whereas the concentration increase with the increase in S_r. Also, the temperature in the boundary layer can be reduced by increasing R / P_r (Figure 11).

Solution obtained in equations (33) and (34) for Sherwood number *Sh* and Nusselt number N_u respectively are shown graphically in Figures.12– 13. It is found that Sherwood number increases with the increase in S_c, and it gets decreased by increasing S_r / R; while on the other hand it rises up with the rise in P_r / R.

4. Conclusion

Effect of Hall parameter on fluid velocity is noticed only for large value of applied magnetic field. Hall parameter *m* can speed up the primary velocity, while it reduces the secondary velocity for $m > k$, where *k* depends on *M*. Both the components of the fluid velocity are increased when the permeability of the porous medium is increased. It is in good agreement with the fact that a porous medium with large porosity enhances the flow through it.

Some other important conclusions noticed are:

- At a particular time the fluid velocity components achieve an extreme value in the region near the plate and then slows down up to free stream value.
- With the increase in radiation parameter; Sherwood number decreases while Nusselt number increases.

- Large value of magnetic field / rotation reduces the primary velocity, and enhances the magnitude of secondary velocity.
- An increase in Soret number causes the decrease in both the component of the Skin friction.

Acknowledgement

Our sincere thanks to the honorable Editor-in-Chief, Professor Aliakbar M. Haghighi; the reviewers; each member of the Editorial Board; and the staff of the Journal 'Application and applied Mathematics' for their valuable comments and suggestions which helped in improving the manuscript.

REFERENCES

Agarwal, H.L., Ram, P.C. and Singh, V. (1983). Combined effect of dissipation and Hall effect on free convective in a rotating fluid, Indian J. Pure ppl. Math., Vol.14(3), pp. 314-332.

Alam, M.S. and Rahman, M.M. (2006). Dufour and Soret effects on mixed convection flow past a vertical porous flat plate with variable suction, Nonlinear Analysis: Modelling and Control, Vol. 11(1), pp. 3-12.

Ali, F., Saqib, M., Khan, I. and Sheikh, N. A. (2019). Heat Transfer Analysis in Ethylene Glycol Based Molybdenum Disulfide Generalized Nanofluid via Atangana-Baleanu Fractional Derivative Approach, Gómez J., Torres L., Escobar R. (eds) Fractional Derivatives with Mittag-Leffler Kernel, Studies in Systems, Decision and Control, Springer, Cham Vol. 194, pp. 217-233.

Anghel, M., Takhar, H. S. and Pop, I.(2000). Dufour and Soret effects on free convection boundary-layer over a vertical surface embedded in a porous medium, Studia Universitatis Babes-Bolyai. Mathematica XLVol. (4), pp. 11-21.

Attia, H.A. (2005). Unsteady couette flow with heat transfer considering ion-slip, Turk J Phys Vol. 29, pp. 379 - 388.

Attia, H.A.(2009). Ion slip effect on unsteady couette flow with heat transfer under exponential decaying pressure gradient, Tamkang Journal of Science and Engineering, Vol. 12(2), pp. 209-214.

Beg, O.A., Bakierand, A. Y. and Prasad, V. R. (2009). Numerical study of free convection magnetohydrodynamic heat and mass transfer from a stretching surface to a saturated porous medium with Soret and Dufour effects, Comp. Materials Science, Vol. 46, pp. 57-65.

Bhargava, R., Sharma, R. and Beg, O. A. (2009). Oscillatory chemically-reacting MHD free convection heat and mass transfer in a porous medium with Soret and Dufour effects: finite element modeling, Int. J. Applied Mathematics and Mechanics Vol. 5(6), pp. 15-37.

Branover, H. (1978). *Magnetohydrodynamic Flow in Ducts*, John Wiley and Sons, New York.

Brewster, M.Q. (1992). *Thermal Radiative Transfer and Properties*, John Wiley & Sons, New York.

Chamkha, A. J. and Rashad, A. M. (2014). Unsteady heat and mass transfer by MHD mixed convection flow from a rotating vertical cone with chemical reaction and Soret and Dufour effects, Canadian Journal of Chemical Engineering, Vol. 92(4), pp. 758-767.

Chamkha, A. J., EL-Kabeir, S. M. M. and Rashad, A. M. (2013). Coupled heat and mass transfer by MHD free convection flow along a vertical plate with streamwise temperature and species concentration variations. Heat Transfer-Asian Research, Vol. 42(2), pp.100-110.

Cowling, T.G. (1957). *Magnetohydrodynamics*, Interscience, New York.

EL-Kabeir, S. M. M., Chamkha, A. J. and Rashad, A. M. (2010). Heat and mass transfer by MHD stagnation-point flow of a power-law fluid towards a stretching surface with radiation, chemical reaction and Soret and Dufour effects, Int. J. Ch. Reactor Engg, Vol. 8, pp. 1-18.

Gangadhar, K. (2013). Soret and Dufour effects on hydro magnetic heat and mass transfer over a vertical plate with a convective surface boundary condition and chemical reaction, Journal of Applied Fluid Mechanics, Vol. 6(1), pp. 95-105.

Gebhart, B. (1961). Transient natural convection from vertical elements, J. Heat Transfer, Vol. 83C, pp. 61-70.

Greenspan, H. P. (1968). *The Theory of Rotating Fluids*, Cambridge University Press, London.

Ibrahim, A.A. (2009). Analytic solution of heat and mass transfer over a permeable stretching plate affected by chemical reaction, internal heating, Dufour-Soret effect and Hall effect, Thermal science, Vol. 13(2), pp. 183-197.

Jaimala, Vikrant and Vivek, K. (2013). Thermal convection in a Couple-Stress fluid in the presence of horizontal magnetic field with Hall currents, Application and applied Mathematics, Vol. 8(1), pp. 161-117.

Kafoussias, N. G. and Williams, E.W. (1995). Thermal-diffusion and diffusion-thermo effects on mixed free-forced convective and mass transfer boundary layer flow with temperature dependent viscosity, International J. of Engineering Science, Vol. 33(9), pp. 1369-1384.

Makinde, O. D. (2011). MHD mixed convection with Soret and Dufour effects past a vertical plate embedded in a porous medium, Latin American Applied Research, Vol. 41, pp. 63-68.

Mazumdar, B.S., Gupta, A.S. and data, N. (1976). Flow and heat transfer in hydrodynamic ekman layer on a porous plate with Hall effects, Int. J. heat mass Transfer, Vol. 19, pp. 523.

Michiyochi, I., Takahashi, I. and Serizawa, A. (1976). Natural convection heat transfer from a horizontal circular cylinder to mercury under a magnetic field, Int. J. Heat Mass Transfer, Vol. 19, pp. 1021-1029.

Muthucumaraswamy, R. and Prema, K. M. A. (2016). Hall effects on flow past an exponentially accelerated infinite isothermal vertical plate with mass diffusion, J. of App. Fluid Mech. Vol. 9(2), pp. 889-897.

Muthucumaraswamy, R., Dhanasekar, N. and Prasad, G. E. (2013). Rotation effects on unsteady flow past an accelerated isothermal vertical plate with variable mass transfer in the presence of chemical reaction of first order, J.of Applied Fluid Mechanics, Vol. 6(4), pp. 485 - 490.

Nield, D.A. and Bejan, A. (2006). *Convection in porous media, third edition,* Springer Science, USA.

Osalusi, E. and Sibanda, P. (2006). On variable laminar convection flow properties due to a porous rotating disk in a magnetic field, Romania J. of Phy., Vol. 51(9 -10), pp. 937 - 950.

Ostrach, S. (1953). An analysis of laminar free convection flow and heat transfer along a flat plate parallel to the direction of the generating body force, NACA report TR-1111, pp. 63-79.

Owen, J. M. and Rogers, R. H. (1989). *Flow and heat transfer in rotating disc systems,* Vol. I, *Rotor - Stator Systems*, John Wiley Sons, New York.

Pohlhausen, E. (1921). Der Warmeaustrausch Zwischen Festen Korpen and Flussigkeiten mit Kleiner Reibung under kleiner Warmeleitung, J. of App. Math. & Mech. (ZAMM) Vol. 1, pp. 115-121.

Pop, I. and Ingham, D.B. (2002*). Transport Phenomena in Porous Media-II,* Pergamon Press, UK.

Postelnicu, A. (2007). Influence of chemical reaction on heat and mass transfer by natural convection from vertical surfaces in porous media considering Soret and Dufour effects, Heat Mass Transfer, Vol. 43, pp. 595-602.

Rajput and Shareef (2018). Study of Soret and Ion slip effects on MHD flow near an Oscillating Vertical Plate in a Rotating System, Applications and Applied Mathematics an International Journal (AAM) Vol. 13(1), pp. 516 – 534.

Rani, H. P. and Reddy, G. J. (2013). Soret and Dufour effects on transient double diffusive free convection of couple-stress fluid past a vertical cylinder, Journal of Applied Fluid Mechanics, Vol. 6(4), pp. 545-554.

Reddy, P. S. and Rao, V. P. (2012). Thermo-Diffusion and Diffusion-Thermo effects on convective heat and mass transfer through a porous medium in a circular cylindrical annulus with quadratic density temperature variation-finite element study, Journal of Applied Fluid Mechanics, Vol. 5(4), pp. 139-144.

Riley, N. (1976). Magnetohydrodynamic free convection about a semi-infinite vertical plate in strong cross-field, J. Appl. Math. Phys. (ZAMP), Vol. 27, pp. 621-631.

Sheikh, N. A., Ali, F., Khan, I. and Gohar, M. (2018). A theoretical study on the performance of a solar collector using CeO_2 and Al_2O_3 water based nanofluids with inclined plate, Atangana–Baleanu fractional model, Chaos, Solitons & Fractals, Vol. 115, pp. 135-142.

Sheikh, N. A., Ali, F., Saqib, M., Khan, I., Jan, S. A. A., Alshomrani, A. S. and Alghamdi, M. S. (2017). Comparison and analysis of the Atangana–Baleanu and Caputo–Fabrizio fractional derivatives for generalized Casson fluid model with heat generation and chemical reaction, Results in Physics, Vol. 7, pp. 789-800.

Siegel, R. (1958). Transient free convection from a vertical flat plate. J. Heat Transfer, Vol. 80, pp. 347-359.

Soong, C. Y. (2001). Thermal buoyancy effects in rotating non-isothermal flows, Int. J. Rotating Machinery, Vol. 7(6), pp. 435-446.

Soong, C. Y. and Ma, H. L. (1995). Unsteady analysis of non-isothermal flow and heat transfer between rotating co-axial disks, Int. J. of Heat and Mass Transfer, Vol. 38(10), pp.1865-1878.

Sparrow, E.M. and Cess, R.D. (1961). The effect of a magnetic field on free convection heat transfer, Int. J. Heat Mass Transfer, Vol. 4, pp. 267-274.

Vafai, K. (2005). *Handbook of porous media, second edition,* Taylor and Francis Group, USA.

Vajravelu, K. and Nayfeh, J. (1992). Hydrodynamics convection at a cone and a wedge, Int. Commun. Heat Mass Transfer, Vol. 19, pp. 701-710.

Watanabe, T. and Pop, I. (1994). Thermal boundary layers in magneto hydrodynamic flow over a flat plate in the presence of transverse magnetic field, Acta. Mech. Vol. 105, pp. 233-238.

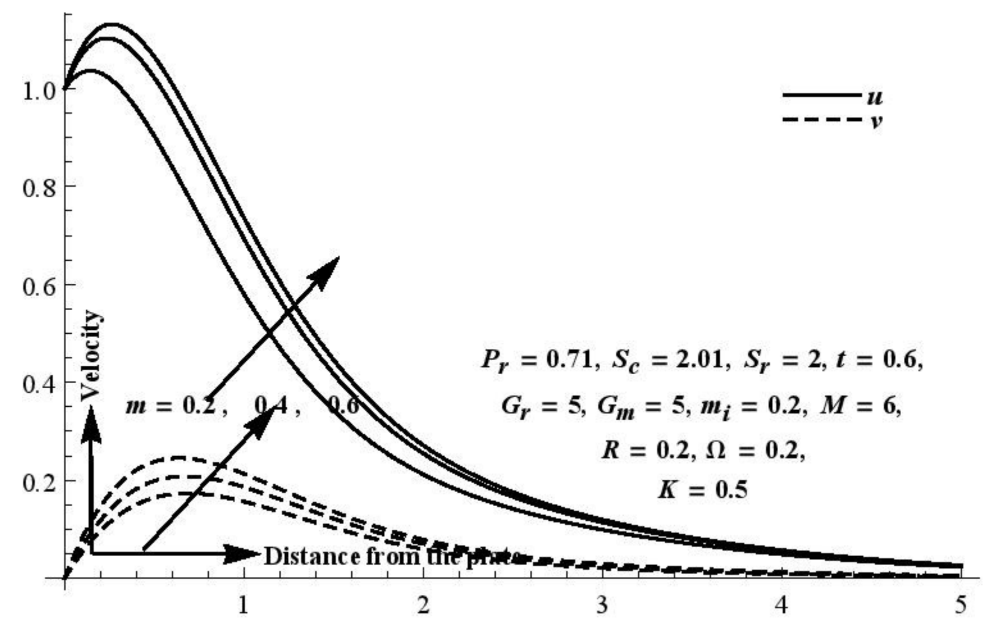

Figure 2. Velocity profile for *m* (< 2) in case 1

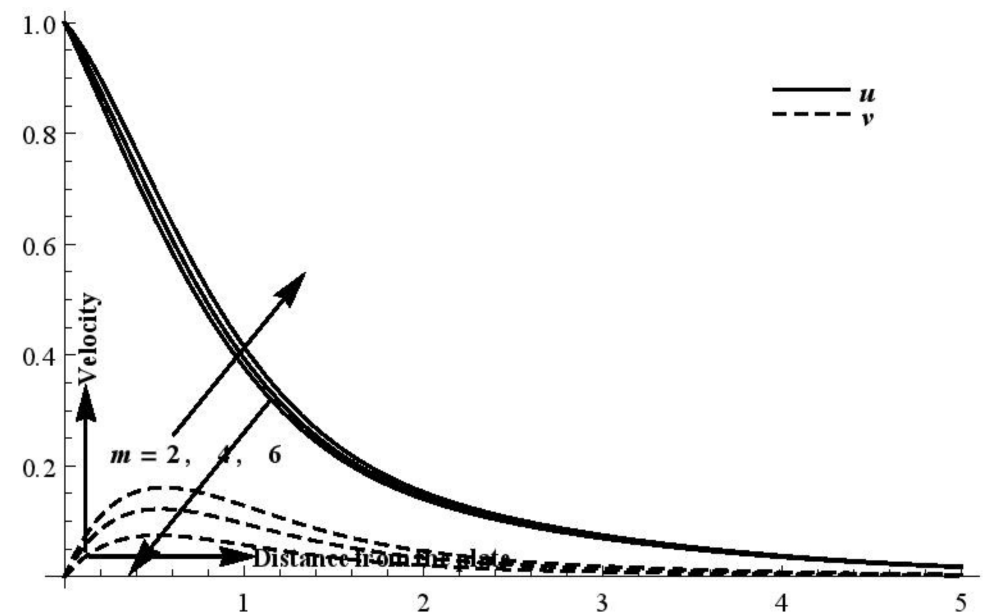

Figure 3. Velocity profile for *m* (≥ 2) in case 1

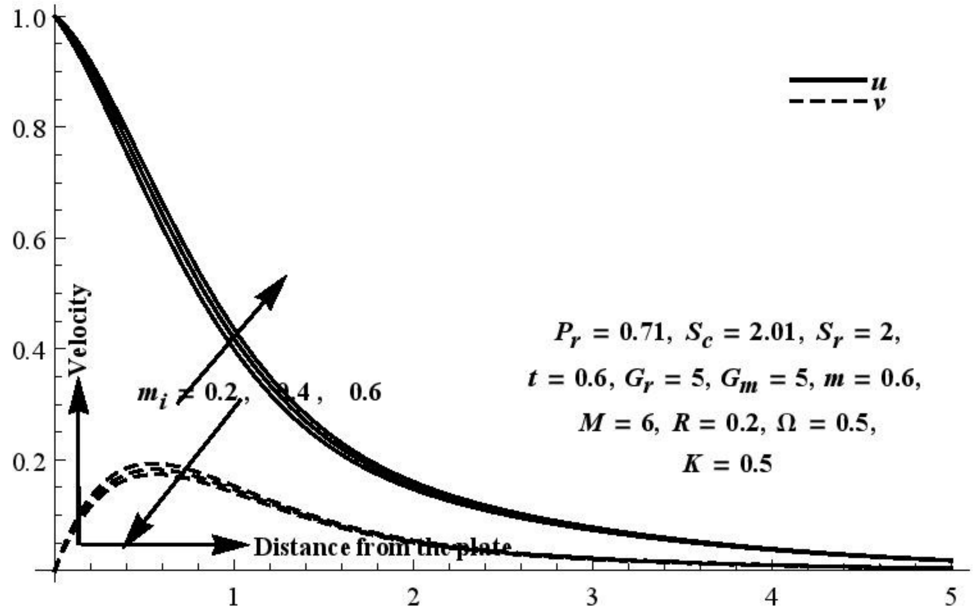

Figure 4. Velocity profile for m_i in case 1

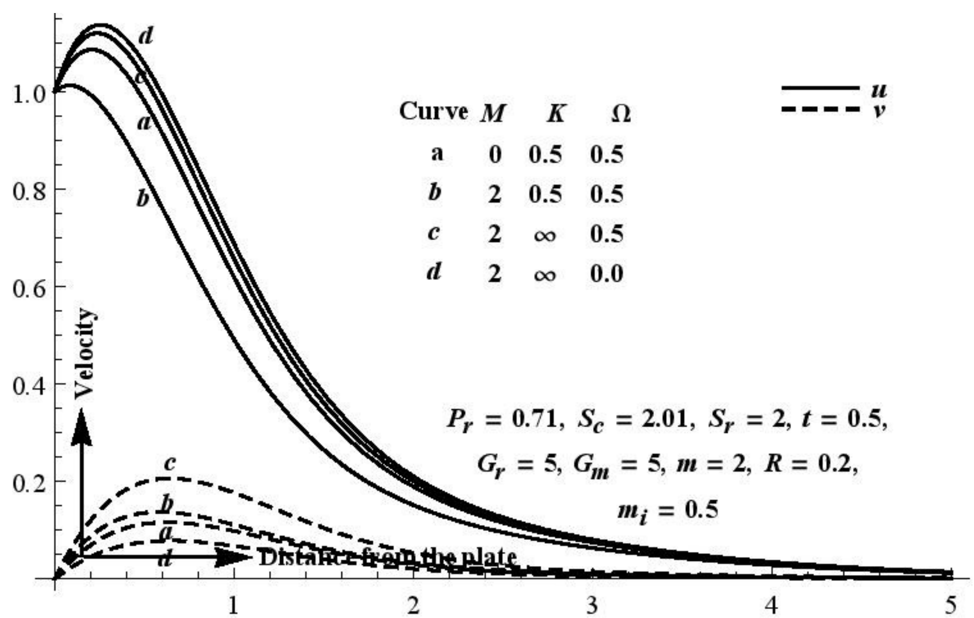

Figure 5. Velocity profile for M, K and Ω in case 1

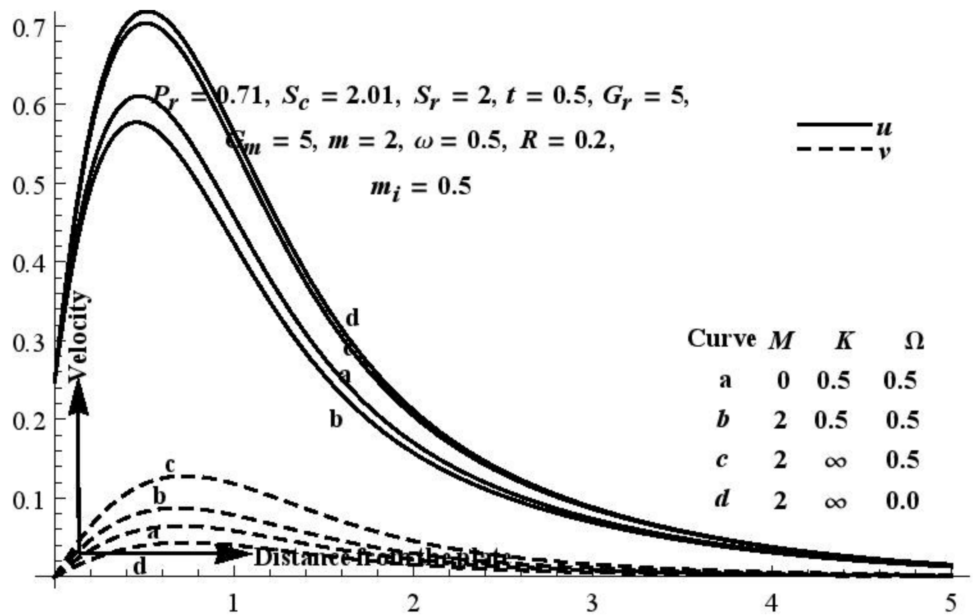

Figure 6. Velocity profile for M, K and Ω in case 2

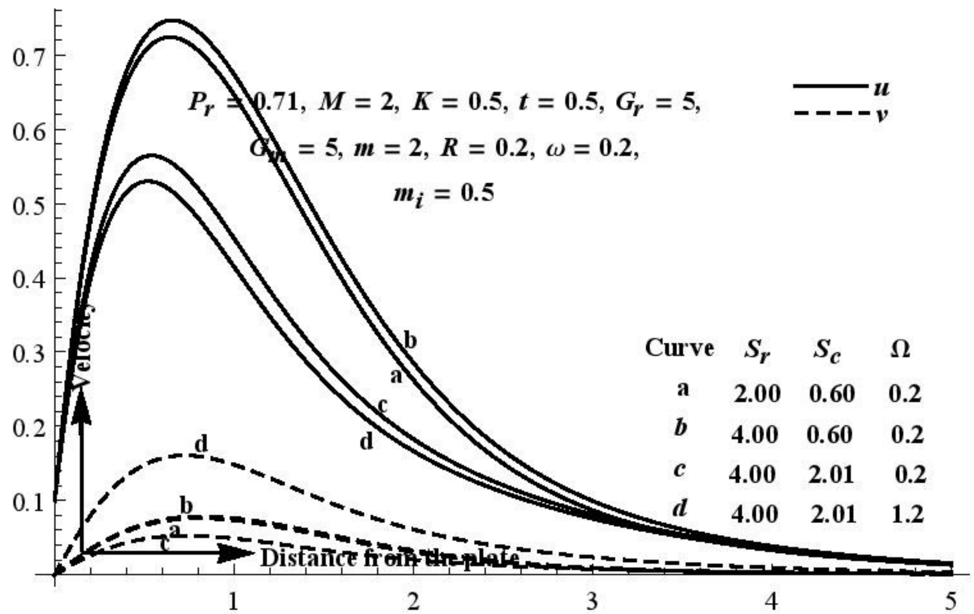

Figure 7. Velocity profile for S_r, S_c and Ω in case 2

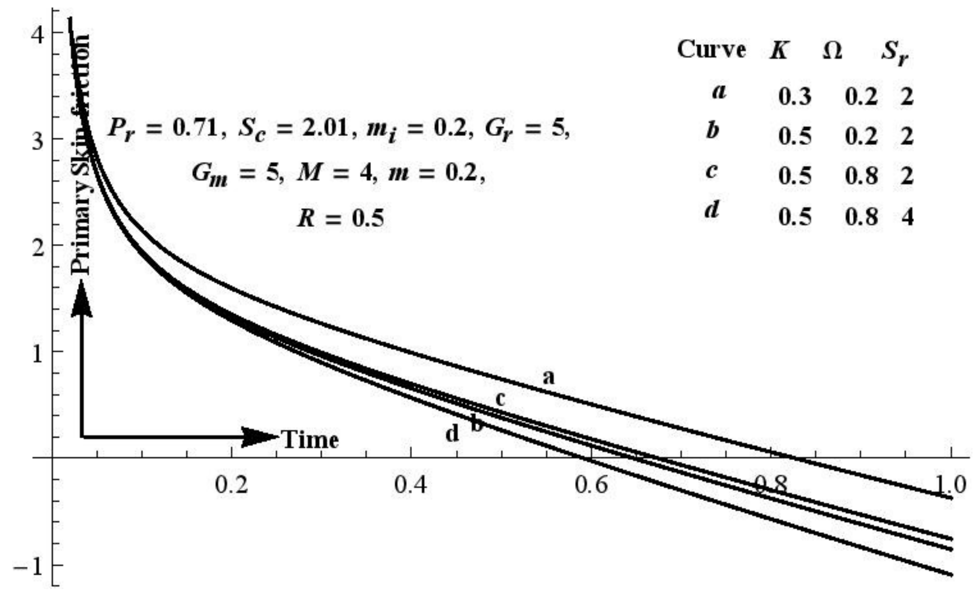

Figure 8. Primary skin friction *K,* Ω and S_r in case 1

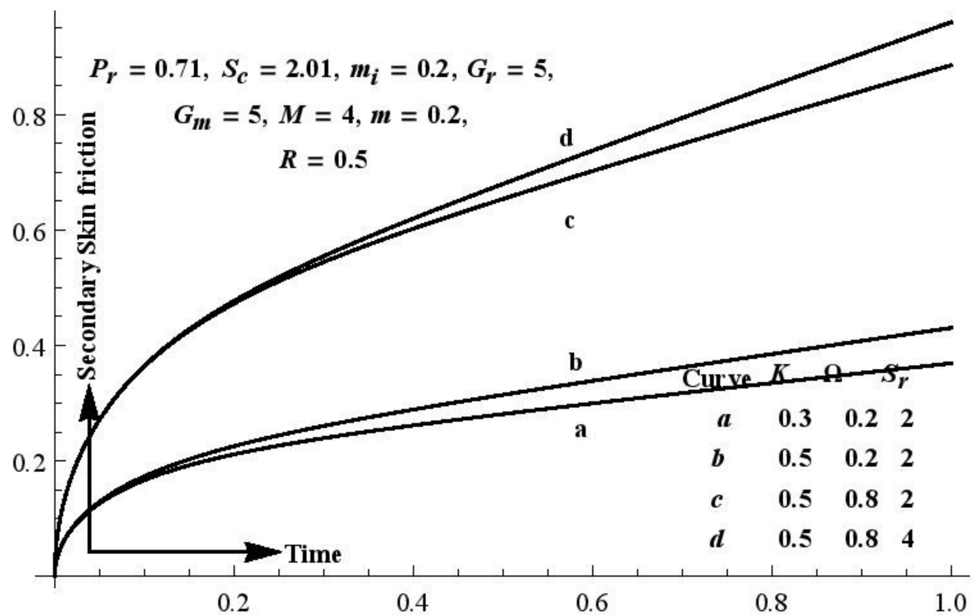

Figure 9. Secondary skin friction *K,* Ω and S_r in case 1

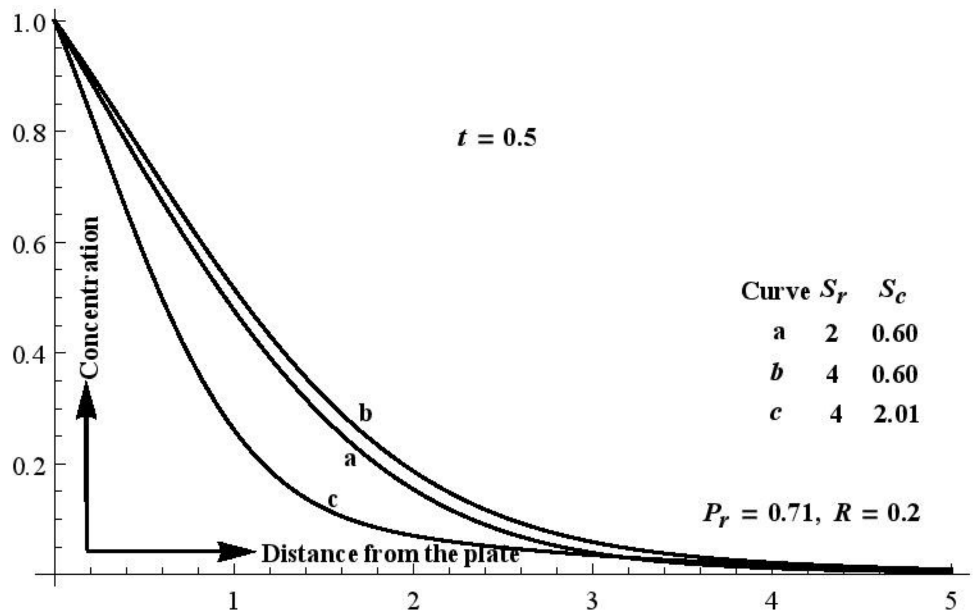

Figure 10. Concentration profile for S_c

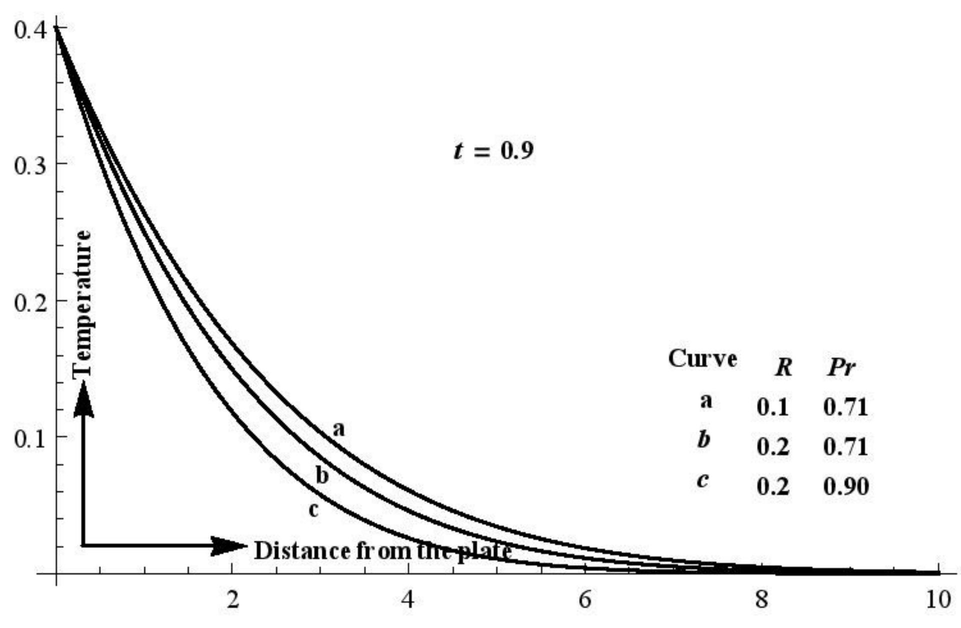

Figure 11. Temperature profile for R

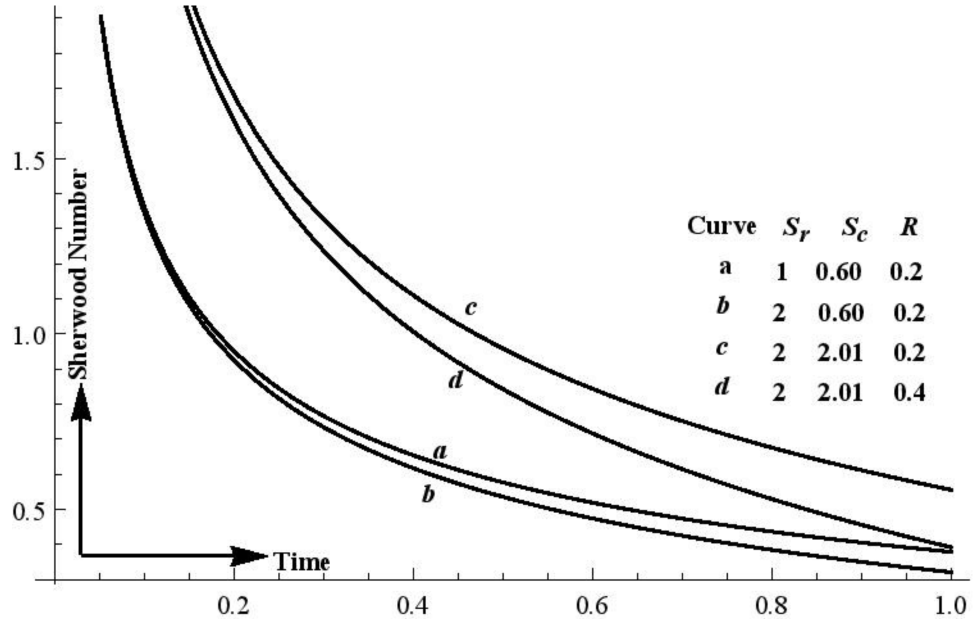

Figure 12. Sherwood number profile with time

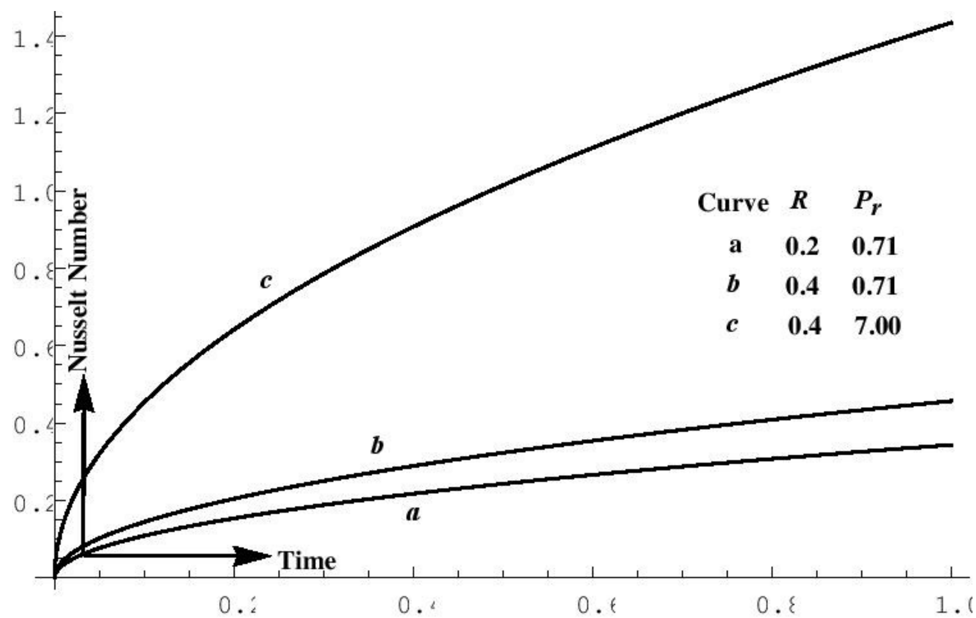

Figure 13. Nusselt number profile with time